

## Comparison of electronic load using linear regulator and boost converter

Razman Ayop<sup>1</sup>, Shahrin Md Ayob<sup>2</sup>, Chee Wei Tan<sup>3</sup>, Tole Sutikno<sup>4</sup>, Mohd Junaidi Abdul Aziz<sup>5</sup>

<sup>1,2,3,5</sup>School of Electrical Engineering, Universiti Teknologi Malaysia, Johor Bahru, Malaysia

<sup>4</sup>Department of Electrical Engineering, Universitas Ahmad Dahlan, Yogyakarta, Indonesia

<sup>4</sup>Embedded System and Power Electronics Research Group, Yogyakarta, Indonesia

---

### Article Info

#### Article history:

Received Mar 12, 2021

Revised Jun 27, 2021

Accepted Jul 13, 2021

---

#### Keywords:

Boost converter

Electronic load

Integral controller

Linear regulator

---

### ABSTRACT

Direct current (DC) electronic load is useful equipment for testing the electrical system. It can emulate various load at a high rating. The electronic load requires a power converter to operate and a linear regulator is a common option. Nonetheless, it is hard to control due to the temperature variation. This paper proposed a DC electronic load using the boost converter. The proposed electronic load operates in the continuous current mode and control using the integral controller. The electronic load using the boost converter is compared with the electronic load using the linear regulator. The results show that the boost converter able to operate as an electronic load with an error lower than 0.5% and response time lower than 13 ms.

*This is an open access article under the [CC BY-SA](https://creativecommons.org/licenses/by-sa/4.0/) license.*



---

### Corresponding Author:

Razman Ayop

School of Electrical Engineering

Faculty of Engineering, Universiti Teknologi Malaysia

81310, UTM Skudai, Johor Darul Takzim, Malaysia

Email: razman.ayop@utm.my

---

## 1. INTRODUCTION

An electronic load is an equipment that can emulate the load. The advantages of using the electronic load are the load can be changed easily and has a high rating. It is a piece of useful equipment in testing electrical system like a battery [1], photovoltaic [2], generator [3], [4], or motor [5] at various load condition. The electronic load is also being used as the dump load to maintain the power quality of an electrical system [3], [6]. The curve tracing of photovoltage (PV) uses the electronic load to determine the degradation level of the PV panel [7]. The electronic load is also being used in surge protection [8]. These examples show that the electronic load is useful in various sector. A commercial electronic load can cost around 500 USD for a 200 W rating and can reach up to 18000 USD for a 6kW rating. Nevertheless, there are some researches available to build an electronic load at a lower cost.

Commonly, the linear regulator is preferred in the direct current (DC) electronic load [1], [9]-[11]. The metal-oxide-semiconductor field-effect transistor (MOSFET) and insulated-gate bipolar transistor (IGBT) is used to emulate the load. This is done by varying the voltage across the gate-source terminal of the MOSFET and the voltage across the gate-emitter terminal of the IGBT. Since the voltage required to control these power switch change with temperature, a closed-loop controller is needed to ensure the electronic load is able to maintain its operation. It also requires a complicated voltage-controlled gate drive. The control becomes more complicated since most of the power dissipation occurs at the power switch that results in high-temperature variation. To overcome this problem, the power switch needs to operate in the saturation

and cut-off regions. This can be achieved by using the load switching method [12]-[15]. Nevertheless, this method requires multiple power switches or resistances, which complicates the control process and this requires closed-loop control.

Since both linear regulator and load switching method requires closed-loop control, a controller is needed. The proportional-integral (PI) controller is commonly used to control the electronic load [1], [12], [16], [17]. There is also the user of the fuzzy logic controller to improve the performance of the electronic load using the PI controller [17]. The proportional-integral-derivative (PID) neural network controller has also been introduced to control the electronic load [18]. Another controller used in the electronic load is the quasi-proportional-resonance controller [19]. These controllers are implemented using an analogue circuit [8], [10] or digital platforms like Arduino [1], [9] or other microcontrollers [12], [16].

The design of the controller and its implementation for the linear regulator and load switching method for the electronic load is complicated. An electronic load with a power converter that can easily be controlled is preferred. The boost converter is one of the switched-mode power supply (SMPS) that can easily be controlled and it is not severely affected by the temperature changes [18]. Nonetheless, this converter is rarely used in the electronic load. Currently, the electronic load using the boost converter does not focus on the passive component design and the control is based on the current-controlled system [20], [21]. The passive component design is important to ensure the electronic load operate properly and within an acceptable ripple. Since the electronic load can receive the current source, the electronic load with the current-controlled system may not work properly. Besides a proper design of electronic load using the boost converter, the comparison between this electronic load with the electronic load using the linear regulator is incomplete in term of accuracy and transient response [13].

This paper presents the design of the DC electronic load using the boost converter. The boost converter is expected to operate in the continuous current mode with the voltage and current ripple below 1%. The results are compared with the electronic load using the linear regulator. Since the linear regulator requires a closed-loop controller, the integral controller is chosen. For a fair comparison, the linear regulator using the boost converter also use the integral controller. The integral controller for both electronic loads is based on resistive feedback to ensure the electronic load is able to work with voltage and current sources. The next section discusses the design of the electronic loads using the linear regulator and boost converter. The next section shows the results and discussions. The last section concludes the result of the comparison.

## 2. DESIGN OF ELECTRONIC LOAD

The DC electronic load consist of several parts. The simple closed-loop DC electronic load is shown in Figure 1. When a DC power source is connected to a DC electronic load, the voltage and current sensors measure the input voltage and current ( $V_i$  and  $I_i$ ), respectively. The  $V_i$  is divided by  $I_i$  to obtain the input resistance,  $R_i$ , based on Ohm's Law. The  $R_i$  is compared with the reference resistance,  $R_{ref}$ , which are set by the user. The  $R_i$  is positive and the  $R_{ref}$  is negative since the increase in control input to the power converter results in the reduction of emulated  $R_i$ . The error produced by comparing the  $R_i$  with the  $R_{ref}$  is fed into an integral controller. Based on the error, the integral controller adjusts the control input for the power converter. The power converter adjusts the operation according to the control input. The process continues until the  $R_i$  is equal to  $R_{ref}$ . There are two power converters used for the DC electronic load, which are the linear regulator and boost converter.

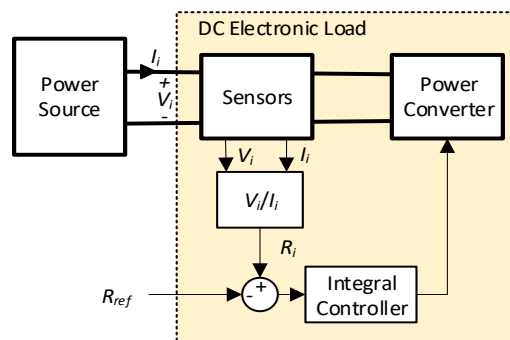


Figure 1. The block diagram of the DC electronic load

**2.1. Linear regulator**

The first power converter for the DC electronic load is the linear regulator. The MOSFET is chosen for the DC electronic load since it is easier to control compared to the transistor. The MOSFET has 3 terminals, which are the drain, source, and gate. The MOSFET is controlled by adjusting the gate-source voltage,  $V_{gs}$ . The higher the  $V_{gs}$ , the higher the drain current,  $I_d$ , that can pass through the MOSFET.

To design the DC electronic load using MOSFET, many characteristics of the MOSFET needs to be considered. The first characteristic is the safe operating zone, as shown in Figure 2. Since the electronic load is DC, the safe operating zone is small. The operation of the DC electronic load needs to maintain within the zone to avoid damaging the MOSFET. The temperature needs to be considered when it comes to the safe operating zone. When the temperature increases, this zone becomes smaller. Therefore, it is recommended to obtain a safe operating zone for the MOSFET at high temperature from the manufacturer. It is also important to install a large heat sink at the MOSFET to reduce the temperature increase at the MOSFET [22].

The I-V characteristic of the MOSFET is controlled by the  $V_{gs}$ . Nonetheless, the  $I_d$  and drain-source voltage,  $V_{ds}$ , also affects the I-V characteristic of the MOSFET, as shown in Figure 3. If the power source connected to the input of the DC electronic load is the voltage source, the  $V_{ds}$  becomes the  $V_i$  when the MOSFET is used in the DC electronic load using the linear regulator. The adjustment of  $V_{gs}$  results in the adjustment of the  $I_d$ . While if the power source connected to the input of the DC electronic load is the current source, the  $I_d$  becomes the  $I_i$  when the MOSFET is used in the DC electronic load using the linear regulator. The adjustment of  $V_{gs}$  results in the adjustment of the  $V_{ds}$ . The  $I_d$ - $V_{ds}$  characteristic also changes when the temperature changes. Therefore, the open-loop operation is not possible since the control input  $V_{gs}$  changes over time.

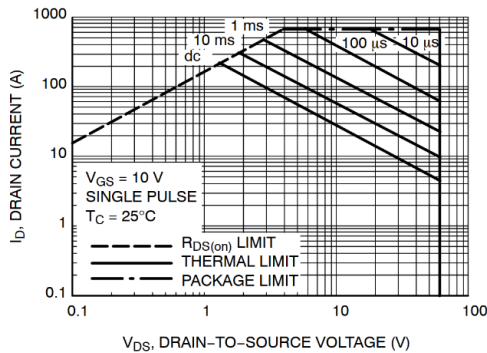


Figure 2. Example of the safe operating zone for the MOSFET at 25 °C [23]

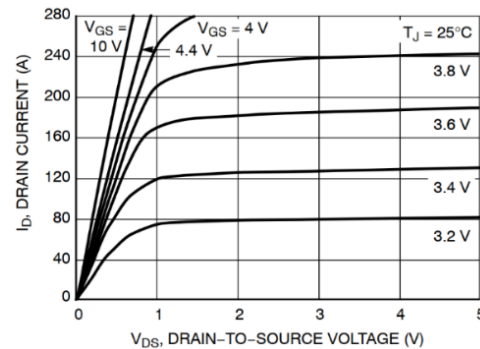


Figure 3. The  $I_d$ - $V_{ds}$  characteristic curve for different  $V_{gs}$  at 25 °C [23]

The design of the DC electronic load is implemented in MATLAB/Simulink, as shown in Figure 4. It is based on the block diagram in Figure 1. There are two components inside the power converter, which are the MOSFET and the controlled voltage source block. Since the simulation does not have a safe operating zone and a proper temperature variation input, these effects cannot be simulated. The integral gain,  $K_i$ , is adjusted manually using the try and error method. Since the MOSFET response quickly, the  $K_i$  can be set at a high value without resulting in an unstable operation. The  $K_i$  chosen is 1000.

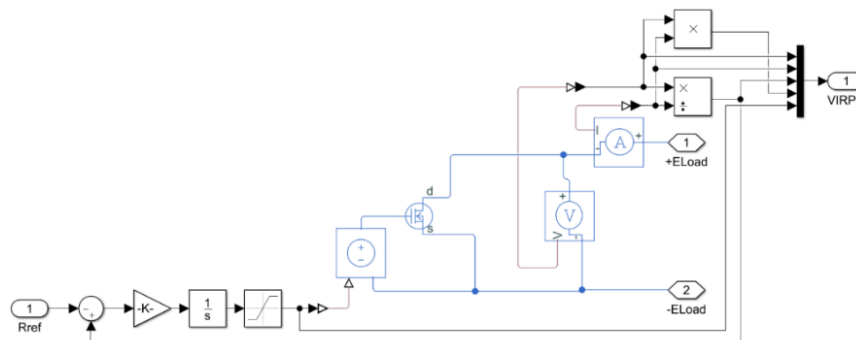


Figure 4. The implementation of the DC electronic load using the MOSFET

## 2.2. Boost converter

The important design step for the linear converter is on the safe operating zone and  $I_d$ - $V_{ds}$  characteristic curve. However, the design of the boost converter shown in Figure 5 focuses on different aspects, which is the duty cycle,  $d$  and ripple [24]. The design consideration on the boost converter is the  $d$ . Since the  $d$  is limited from 0 to 1, a proper design of the  $R_o$  is crucial to avoid the operation outside the  $d$  limit. The boost converter is chosen from the SMPS category due to its low number of components and low  $I_i$  ripple. This is an important characteristic because the ideal DC electronic load should not have ripples. Nonetheless, the power converter under the SMPS category contains current or voltage ripples. Therefore, it is essential to choose the power converter with the low ripple, especially at the  $V_i$  and  $I_i$ . The control input from the integral controller is the  $d$  and it is converted into switching pulse,  $p_s$ , by the pulse width modulation, PWM.

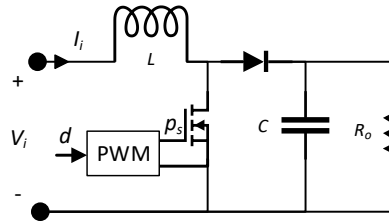


Figure 5. The circuit diagram of the boost converter

The  $d$ - $R_o$  relationship is crucial when using the boost converter for the DC electronic load. This relationship is shown in (1) [24]. In an ideal condition, the  $d$  is “0 to 1”. However, the boost converter unable to follow this range due to the nonideality factor [25]. It is recommended that the operation of the boost converter is “0.10 to 0.75” to avoid voltage regulation problem. This is because when the  $d$  is above 0.75, the output voltage,  $V_o$ , begins to drop and affect the performance of the electronic load. Therefore, the minimum and maximum  $d$  ( $d_{min}$  and  $d_{max}$ ) are 0.10 and 0.75, respectively. Then, the minimum and maximum  $R_i$  ( $R_{i_{min}}$  and  $R_{i_{max}}$ ) need to be chosen. The  $R_{i_{min}}$  and  $R_{i_{max}}$  become the range of emulated resistance for the DC electronic load. The  $R_{i_{min}}$  and  $R_{i_{max}}$  need to obey the range in (2) [24]. In this design, the  $R_{i_{min}}$  and  $R_{i_{max}}$  are set to 10 and 100, respectively and the range obey (2). Then, the  $R_o$  is chosen within the range of (2).

$$R_o = \frac{R_i}{(1-d)^2} \quad (1)$$

$$\frac{R_{i_{max}}}{(1-d_{min})^2} \leq R_o \leq \frac{R_{i_{min}}}{(1-d_{max})^2} \quad (2)$$

$$V_i = \sqrt{P_{R_o} R_i} \quad (3)$$

The list of parameters is tabulated in Table 1. Since most of the power is transmitted to  $R_o$ , it is essential to ensure the  $R_o$  capable to handle the power. The power transmitted to  $R_o$ ,  $P_{R_o}$ , is calculated using (3) [24]. The rating of the  $R_o$  is highly depended on the  $V_i$ , which is the voltage rating of the DC electronic load, and the  $R_i$ . Note that the rating of  $V_i$  is based on  $R_i$  and  $P_{R_o}$ . Therefore, the chosen  $R_o$  is 130  $\Omega$  (within the range of 123.5  $\Omega$  and 160.0  $\Omega$ ).

Table 1. The desired specification and calculated parameters for the DC electronic load using the boost

Parameter	Value
Minimum Input Resistance, $R_{i_{min}}$	10 $\Omega$
Maximum Input Resistance, $R_{i_{max}}$	100 $\Omega$
Minimum Duty Cycle, $D_{min}$	0.10
Maximum Duty Cycle, $D_{max}$	0.75
Maximum Input Voltage, $V_{i_{max}}$	50 V
Switching Frequency, $f_s$ (kHz)	100 kHz
Output Voltage Ripple Factor, $\gamma_{V_o}$	1%
Input Current Ripple Factor, $\gamma_{I_i}$	1%
Output Resistance, $R_o$	130 $\Omega$
Inductance, $L$ (mH)	19.26 mH
Capacitance, $C$ ( $\mu$ F)	5.56 $\mu$ F

A resistive load does not produce any voltage and current ripple. Nonetheless, the boost converter contains ripples and cannot be eliminated. To remove the current ripple at  $I_i$ , the inductance,  $L$ , chosen needs to be infinity. The infinity  $L$  is an impractical solution and results in a slow transient. Therefore, a 1%  $I_i$  ripple factor,  $\gamma_{Ii}$ , is chosen since it is accurate enough to produce a steady current. The  $L$  is calculated using (4) [24], which equals to 19.26 mH. Although the  $V_o$  ripple factor,  $\gamma_{Vo}$ , can be ignored since this parameter is not considered in the DC electronic load, it still essential to avoid unstable operation. The  $\gamma_{Vo}$  is calculated using (5) [24], which equals to 5.56  $\mu$ F.

$$L = \frac{4R_o}{27\gamma_{Ii}f_s} \quad (4)$$

$$C = \frac{1}{\gamma_{Vo}f_s} \left( \frac{1}{R_o} - \sqrt{\frac{R_{i,min}}{R_o^3}} \right) \quad (5)$$

Since the boost converter consists of an inductor and capacitor, the transient response is much slower compared to the linear regulator. Therefore, the  $K_i$  is adjusted properly to ensure the stability of the electronic load. Using the try and error method, the chosen  $K_i$  is 3. The design of boost converter is then implemented into MATLAB/Simulink, as shown in Figure 6.

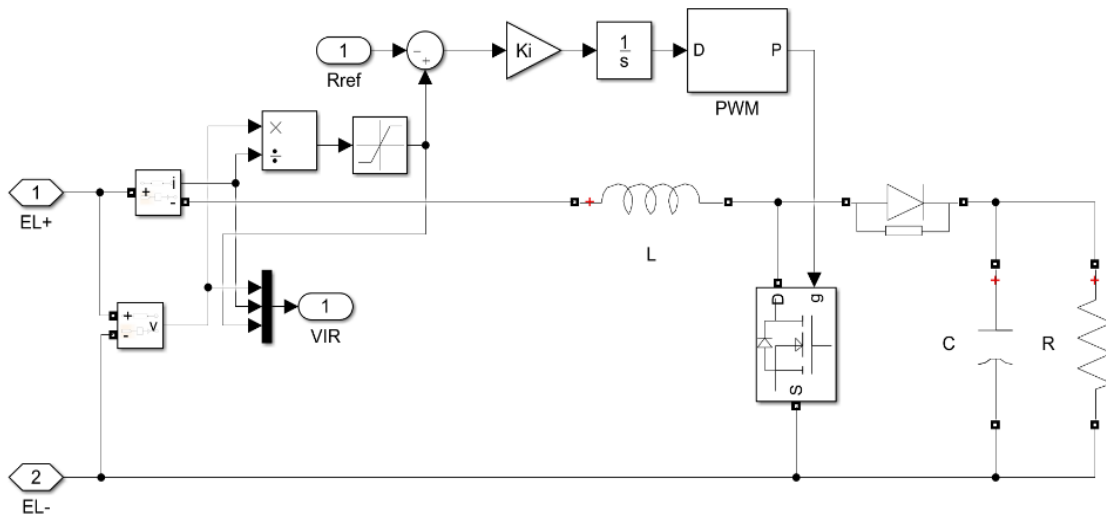


Figure 6. The implementation of the DC electronic load using the boost converter.

### 3. RESULTS AND DISCUSSION

A high accuracy emulation of the load is important for the DC electronic load. The lower the percentage error,  $e\%$ , the higher the accuracy. The  $e\%$  is calculated using (6). The DC electronic loads using the linear regulator and boost converter are simulated separately with  $R_{ref}$  from 10  $\Omega$  to 100  $\Omega$ . Both electronic loads are connected to the 100 V voltage source. The  $V_i$  and  $I_i$  are measured to determine  $R_i$ . The  $e\%$  obtained at various  $R_{ref}$  are visualized in Figure 7. The results show that the electronic load using the linear regulator has a lower  $e\%$  compared to the electronic load using the boost converter. This means that the electronic load using the linear regulator has higher accuracy compared to the electronic load using the boost converter. This effect is caused by the  $I_i$  ripple present in the boost converter. According to [24], the highest ripple occur when the  $R_i$  is 4/9 out of  $R_o$ . Since  $R_o$  is 130  $\Omega$ , the highest  $I_i$  occur when  $R_i$  equals to 57.78  $\Omega$ . Based on Figure 7, it is clearly shown that  $e\%$  is the highest doing that condition. Therefore, the  $I_i$  ripple affects the accuracy of the electronic load using the boost converter.

$$e\% = \frac{|R_i - R_{ref}|}{R_{ref}} \times 100\% \quad (6)$$

For the electronic load using the linear regulator, the result shows that the  $e\%$  becomes higher when the  $R_{ref}$  increases. Nonetheless, it is significantly lower compared to the electronic load using the boost

converter. It is worth mention that the simulation does not consider the effect of temperature variation and electrical noise. As mention before, the  $V_{gs}$  requires to emulate load changes with time. Therefore, it is harder to control the electronic load and may result in a higher error. The slight change of  $V_{gs}$  also affects the emulation of the load. Therefore, the electrical noise in the  $V_{gs}$  may significantly affect the accuracy of the electronic load using the linear regulator. The hardware implementation is required to analyst this effect, which is out of the scope of the study.

The electronic load using the linear regulator and boost converter are simulated separately with the  $R_{ref}$  is stepped-up from  $20\ \Omega$  to  $80\ \Omega$  at  $0.03\ \text{s}$  and stepped-down from  $80\ \Omega$  to  $20\ \Omega$  at  $0.06\ \text{s}$ . The simulation is conducted to ensure the electronic load transient response does not affect the experimental result during load emulation. The desired response for the electronic load is the  $I_i$  changes instantaneously. By referring to Figure 8, the electronic load using the linear regulator able to change instantaneously. However, the electronic load using the boost converter has a slow transient response. Assume that the steady-state time,  $t_s$ , is defined as the time taken for the parameter to achieve within 2% of its final value, the  $t_s$  during stepped-up load is  $9.2\ \text{ms}$ . While the  $t_s$  during stepped-down load is  $12.9\ \text{ms}$ .

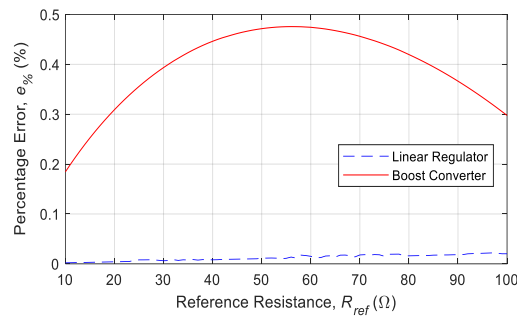


Figure 7. The  $e\%$  against  $R_{ref}$  for the linear regulator and boost converter in the DC electronic load application

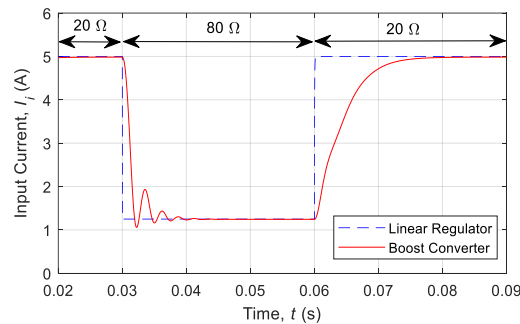


Figure 8. The transient response of  $I_i$  when the load is stepped-up from  $20\ \Omega$  to  $80\ \Omega$  and stepped-down from  $80\ \Omega$  to  $20\ \Omega$

The delay during the load change is insignificant if the power converter connected to the electronic load has a slow response. However, the load emulation becomes inaccurate if the power converter connected to the electronic load has a faster response compared to the electronic load. The slow response is due to the requirement of the boost converter to have a large  $L$ , which reduced the  $I_i$  ripple. To avoid this problem, a higher  $f_s$  is needed. Nonetheless, it may result in a higher switching loss. Which increase the heat generation at the power switch in the boost converter. If the transient response result is not collected for the experiment, the proposed electronic load can be applied to the experiment.

The power dissipation for the boost converter is mostly at the resistance. While the power dissipation for the linear regulator is mostly at the MOSFET. This is an undesired situation especially for high power load emulation since the MOSFET has limited safe operating area, especially during DC operation. The temperature is also a problem faced by the linear regulator based electronic load. Since the power dissipates mostly at the MOSFET, the temperature of the MOSFET increases significantly. This may lead to the failure of the MOSFET and the operation of the electronic load stops. The temperature increase also changes the  $V_{gs}$  significantly, thus a closed-loop system is needed to maintain the emulation of the load.

#### 4. CONCLUSION

In general, the boost converter able to be used as the DC electronic load. Since the temperature is not significantly affecting the operating point, the open-loop system is an option. The power dissipation is located to the output resistance and not at the power switch. However, the electronic load using the boost converter is inferior compared to the electronic load using the linear regulator. When the temperature and electrical noise effects are discounted, the accuracy of the electronic load using the boost converter is lower compared to the electronic load using the linear regulator. This is due to the current ripple problem faced by the boost converter. The transient response of the electronic load using the boost converter is lower compared to the electronic load using the linear regulator. This is due to the large inductor needed to maintain a low current ripple. To summarize, the boost converter is suitable to be implemented for the DC electronic load. Nonetheless, it has lower accuracy and slower response when compared with the linear regulator.

#### ACKNOWLEDGEMENTS

The authors would like to express gratitude to Universiti Teknologi Malaysia (UTM) for providing comprehensive library facilities and funding. Funding provided by Universiti Teknologi Malaysia Encouragement Research Grant under vote Q.J130000.2651.18J39. Lastly, thanks to colleagues who have either directly or indirectly contributed to the completion of this work.

#### REFERENCES

- [1] K. Lawsri, and S. Po-Ngam, "DC electronics load for AH battery testing," in *2017 International Electrical Engineering Congress (iEECON)*, 2017, pp. 1-4, doi: 10.1109/IEECON.2017.8075894.
- [2] P. Papageorgasa, D. Piromalisb, T. Valavanisa, S. Kambasisa, T. Iliopouloua, and G. Vokasa, "A low-cost and fast PV IV curve tracer based on an open source platform with M2M communication capabilities for preventive monitoring," *Energy Procedia*, vol. 74, pp. 423-438, 2015, doi: 10.1016/j.egypro.2015.07.641.
- [3] U. ur Rehman, and M. Riaz, "Design and implementation of electronic load controller for small hydro power plants," in *2018 Int. Conf.e on Comp., Math. and Eng. Tech.s (iCoMET)*, 2018, pp. 1-7, doi: 10.1109/ICOMET.2018.8346450.
- [4] R. Pudur, and V. K. Srivastava, "Performance study of electronic load controller for integrated renewable sources," in *2018 2nd International Conference on Electronics, Materials Engineering & Nano-Technology (IEMENTech)*, 2018, pp. 1-6, doi: 10.1109/IEMENTECH.2018.8465144.
- [5] Q. Yang, H. Yang, X. Gu, S. He, and Z. Cai, "Power electronic load system for motor drivers testing considering motor faulty status simulation," in *2019 22nd International Conference on Electrical Machines and Systems (ICEMS)*, 2019, pp. 1-6, doi: 10.1109/ICEMS.2019.8921962.
- [6] R. R. Singh, B. A. Kumar, D. Shruthi, R. Panda, and C. T. Raj, "Review and experimental illustrations of electronic load controller used in standalone Micro-Hydro generating plants," *Engineering Science and Technology, an International Journal*, vol. 21, pp. 886-900, 2018, doi: 10.1016/j.jestch.2018.07.006.
- [7] A. A. Willoughby, and M. O. Osinowo, "Development of an electronic load I-V curve tracer to investigate the impact of Harmattan aerosol loading on PV module performance in southwest Nigeria," *Solar Energy*, vol. 166, pp. 171-180, 2018, doi: 10.1016/j.solener.2018.03.047.
- [8] S. Wongcharoen, S. Deeon, and N. Mungkung, "Application of electronic load circuit for electrical safety by using a serial mode comparator," *Przegląd Elektrotechniczny*, vol. 96, pp. 17-22, 2020, doi: 10.15199/48.2020.04.03.
- [9] N. Saini, A. Mudgal, K. Kumar, J. Srivastava, and V. Dutta, "Design of microcontroller based I-V plotter using IGBT electronic load," in *2016 IEEE 1st International Conference on Power Electronics, Intelligent Control and Energy Systems (ICPEICES)*, 2016, pp. 1-5, doi: 10.1109/ICPEICES.2016.7853530.
- [10] J. Peng, Y. Chen, Y. Fang, and S. Jia, "Design of programmable DC electronic load," in *2016 International Conference on Industrial Informatics-Computing Technology, Intelligent Technology, Industrial Information Integration (ICIICII)*, 2016, pp. 351-355, doi: 10.1109/ICIICII.2016.0090.
- [11] V.-M. Placinta, F. Babarada, C. Ravariu, and L. G. Alecu, "Digitally controlled electronic load for testing power supplies reliability," *Roumaine Des Sciences Techniques-Serie Electrotechnique Et Energetique*, vol. 64, pp. 131-136, 2019.
- [12] A. Shiqi, "High power DC electronic load," in *2017 Chinese Automation Congress (CAC)*, 2017, pp. 1698-1701, doi: 10.1109/CAC.2017.8243041.
- [13] W. Jiang, J. Wang, Q. Wang, S. Xu, S. Hashimoto, and Z. Liu, "Design and implementation of a low-power low-cost digital current-sink electronic load," *Energies*, vol. 12, p. 2611, 2019, doi: 10.3390/en12132611.
- [14] V. K. Murali, and V. Sandeep, "Design and simulation of current sensor based electronic load controller for small scale three phase self excited induction generator system," *International Journal of Renewable Energy Research (IJRER)*, vol. 10, pp. 1638-1644, 2020.
- [15] B. N. Roodsari, and E. P. Nowicki, "Analysis and experimental investigation of the improved distributed electronic load controller," *IEEE Transactions on Energy Conversion*, vol. 33, no. 3, pp. 905-914, Sept. 2018, doi: 10.1109/TEC.2018.2823334.
- [16] Z. Meng-Ting, W. Ming-Yan, and W. Le-San, "Design and implementation of a multifunctional DC electronic load," in *2017 IEEE Transportation Electrification Conference and Expo, Asia-Pacific (ITEC Asia-Pacific)*, 2017, pp. 1-6, doi: 10.1109/ITEC-AP.2017.8080808.

- [17] E. Mishra, and S. Tiwari, "Comparative analysis of fuzzy logic and PI controller based electronic load controller for self-excited induction generator," *Advances in Electrical Engineering*, vol. 2017, p. 5620830, 2017, doi: 10.1155/2017/5620830.
- [18] H. K. Khleaf, A. K. Nahar, and A. S. Jabbar, "Intelligent control of DC-DC converter based on PID-neural network," *International Journal of Power Electronics and Drive Systems*, vol. 10, pp. 2254-2262, 2019, doi: 10.11591/ijpeds.v10.i4.pp2254-2262.
- [19] P. Chen, and F. Wu, "Research and implementation of single-phase AC electronic load based on quasi-PR control," in *2018 International Conference on Advanced Mechatronic Systems (ICAMEchS)*, 2018, pp. 157-161, doi: 10.1109/ICAMEchS.2018.8507104.
- [20] H. C. Kanchev, "Modeling of boost converter-based electronic load with energy recycling capability," in *2018 IX National Conference with International Participation (ELECTRONICA)*, 2018, pp. 1-4, doi: 10.1109/ELECTRONICA.2018.8439666.
- [21] A. Asbayou, M. Agdam, A. Aamoume, A. Soussi, A. Ihla, and L. Bouhouch, "Utilization of MOSFET transistor as an electronic load to trace IV and PV curve of a solar panel," in *E3S Web of Conferences*, 2021, p. 01021, doi: 10.1051/e3sconf/202122901021.
- [22] T. Nujithra, and U. S. Premarathne, "Investigation of efficient heat dissipation mechanisms for programmable DC electronic load design," in *2018 8th International Conference on Power and Energy Systems (ICPES)*, 2018, pp. 201-206, doi: 10.1109/ICPESYS.2018.8626879.
- [23] O. Semiconductor, "NTB5860NL, NTP5860NL, NVB5860NL N-Channel MOSFET 60 V, 220 A," O. Semiconductor, Ed., ed, 2012.
- [24] R. Ayop, and C. W. Tan, "Design of boost converter based on maximum power point resistance for photovoltaic applications," *Solar Energy*, vol. 160, pp. 322-335, 2018, doi: 10.1016/j.solener.2017.12.016.
- [25] D. W. Hart, *Power Electronics*, Valparaiso University, Indiana: Tata McGraw-Hill Education, 2011.

## BIOGRAPHIES OF AUTHORS



**Razman Ayop** received the Bachelor's degree in electrical engineering with first-class honors, the master's degree in electrical engineering with specialization in power system, and the Ph.D. degree in electrical engineering from Universiti Teknologi Malaysia (UTM), Johor, Malaysia, in 2013, 2015, and 2018, respectively. He is a Senior Lecturer with UTM and a member of Power Electronics and Drives Research Group, School of Electrical Engineering, Faculty of Engineering, UTM. His research interests include renewable energy and power electronics



**Shahrin bin Md. Ayob** was born in Kuala Lumpur, Malaysia. He obtained his first degree in Electrical Engineering, Master in Electrical Engineering (Power), and Doctor of Philosophy (Ph.D.) from Universiti Teknologi Malaysia in 2001, 2003, and 2009, respectively. Currently, he is an associate professor at the School of Electrical Engineering, Faculty of Engineering, Universiti Teknologi Malaysia. He is a registered Graduate Engineer under the Board of Engineer Malaysia (BEM) and Senior Member of IEEE. His current research interest is the solar photovoltaic system, electric vehicle technology, fuzzy system, and evolutionary algorithms for power electronics applications.



**Chee Wei, Tan** (M'11–SM'17) received his B.Eng. degree in Electrical Engineering (First Class Honors) from Universiti Teknologi Malaysia (UTM), in 2003 and a Ph.D. degree in Electrical Engineering from Imperial College London, London, U.K., in 2008. He is currently an associate professor at Universiti Teknologi Malaysia and a member of the Power Electronics and Drives Research Group, School of Electrical Engineering, Faculty of Engineering. His research interests include the application of power electronics in renewable/alternative energy systems, control of power electronics and energy management system in microgrids. He is also a Chartered Engineer registered with Engineering Council, UK, a professional engineer registered with Board of Engineers Malaysia and a professional technologist registered with Malaysia Board of Technologists. He is actively participating in IEEE activities and conferences, which he is also the chair of the IEEE Power Electronic Society (PEL) Malaysia Chapter for year 2018. He was awarded the Malaysia Research Start Award (High Impact Paper – Engineering and Technologies) 2018 by the Ministry of Education Malaysia.





**Tole Sutikno**, Associate Professor in Electrical and Computer Engineering, Ahmad Dahlan (UAD) University, Yogyakarta, Indonesia. He received his B.Eng., M.Eng. and Ph.D. degree in Electrical Engineering from Diponegoro University (Semarang, Indonesia), Universitas Gadjah Mada (Yogyakarta, Indonesia) and Universiti Teknologi Malaysia (Johor, Malaysia), in 1999, 2004 and 2016, respectively. He has been an Associate Professor in UAD, Yogyakarta-Indonesia since 2008. His research interests include the field of power electronics, industrial applications, industrial electronics, industrial informatics, motor drives, FPGA applications, intelligent control and digital library.



**Mohd Junaidi Abdul Aziz** was born in Kuala Terengganu, Malaysia, in 1979. He received his B.S. and M.S. degrees in Electrical Engineering from the Universiti Teknologi Malaysia (UTM), Kuala Lumpur, Malaysia, in 2000 and 2002, respectively; and his Ph.D. in Electrical Engineering from The University of Nottingham, Nottingham, England, UK, in 2008. Currently working as Associate Professor, Faculty of Electrical Engineering, UTM. His current research interests include power electronics converter, battery management system in electric vehicles and battery charger.